Pan-cancer analyses reveal molecular and clinical characteristics of cuproptosis regulators in cancer

Changwu Wu
Department of Neurosurgery, Xiangya Hospital, Central-South University, Changsha, China
Jun Tan
Department of Neurosurgery, Xiangya Hospital, Central-South University, Changsha, China
Xiangyu Wang
Department of Neurosurgery, Xiangya Hospital, Central-South University, Changsha, China
Chaoying Qin
Department of Neurosurgery, Xiangya Hospital, Central-South University, Changsha, China
Wenyong Long
Department of Neurosurgery, Xiangya Hospital, Central-South University, Changsha, China
Yimin Pan
Department of Neurosurgery, Devision of Experimental Neurosurgery, University of Heidelberg, Im Neuenheimer Feld 400, 69120 Heidelberg, Germany
Yuzhe Li
Department of Neurosurgery, Xiangya Hospital, Central-South University, Changsha, China
Qing Liu (liuqingdr@csu.edu.cn)
Department of Neurosurgery, Xiangya Hospital, Central-South University, Changsha, China

Research Article

Keywords: cuproptosis, pan-cancer, fatty acid metabolism, drug sensitivity, immunotherapy

Posted Date: May 13th, 2022

DOI: https://doi.org/10.21203/rs.3.rs-1652748/v1

Version of Record: A version of this preprint was published at iMeta on December 5th, 2022. See the published version at https://doi.org/10.1002/imt2.68.

Abstract

Imbalance in copper homeostasis can be lethal to the body. A recent study found that excess copper induces cell death in a way that has never been characterized before, which is dependent on mitochondrial stress and referred to as “cuproptosis.” The role of cuproptosis in tumors has not yet been elucidated. In this study, we revealed the complex and important roles of cuproptosis regulators and cuproptosis activity in tumors via a comprehensive analysis of multi-omics data from more than 10 000 samples of 33 tumor types. We found that the cyclin-dependent kinase inhibitor 2A is the most frequently altered cuproptosis regulator, and the cuproptosis regulator expression is dysregulated in various tumors. Additionally, we developed a cuproptosis activity score to reflect the overall cuproptosis level. Based on the expression levels of cuproptosis regulators, tumors can be divided into two clusters with different cuproptosis activities and survival outcomes. Importantly, cuproptosis activity was found to be associated with the prognosis of multiple tumors and multiple tumor-related pathways, including fatty acid metabolism and remodeling of the tumor microenvironment. Furthermore, cuproptosis extensively increased the sensitivity to multiple drugs and exhibited potential to predict the outcome of immunotherapy. We also comprehensively identified cuproptosis-related microRNAs, long non-coding RNAs, and transcription factors. In summary, this study reveals important molecular and clinical characteristics of cuproptosis regulators and cuproptosis activity in tumors, and suggests the use of cuproptosis as a promising tumor therapeutic approach. This study provides an important reference point for future cuproptosis-related research.

Introduction

Transition metals are essential for complex biochemical reactions in the human body.[1] Copper (Cu), a trace metal element, is important for the maintenance of normal cellular biological functions.[2,3] Cu is also involved in various cellular processes closely related to cell fate, such as oxidative phosphorylation, aerobic respiration, and cell growth and development, in humans.[3−8] Maintaining balanced Cu homeostasis is critical to the body, and even small changes in Cu homeostasis can cause irreversible and serious damage.[1,9] The most representative diseases caused by dysregulation of Cu metabolism are Wilson’s disease, caused by the excessive accumulation of Cu in the liver due to defects in the transporter protein, ATPase copper transporting beta,[9] and Menkes’ disease, caused by severe Cu deficiency resulting from difficulties in Cu release from the enterocyte to the bloodstream due to mutations in ATPase copper transporting beta.[9−11] In addition, the role of Cu in cancer has attracted significant attention in research. Many studies have reported the accumulation of Cu in the serum samples of patients with cancer, including breast cancer,[12] lung cancer,[13] and hepatocellular carcinoma.[14] Mouse-based models of hepatocellular carcinoma have also demonstrated significantly elevated levels of Cu in tumor tissues.[15] Although there is a common tendency for Cu accumulation in tumors, the association between Cu levels and cancer risk is unknown.[7] However, Cu has been shown to be important for tumor proliferation and angiogenesis,[16,17] which may explain the enrichment of Cu in tumor tissue regions. Accumulation of Cu is observed in the nuclear region of cancer cells.[18] Based on this, Cu chelators have been shown to inhibit

tumor growth and angiogenesis.[17] For example, trientine significantly inhibits tumor development in human hepatocellular carcinoma cell lines,[19] while tetrathiomolybdate inhibits tumor growth in melanoma cell lines resistant to BRAF or mitogen-activated protein kinase kinase-1/2 inhibitors.[20]

Excessive Cu is toxic to cells,[21] which explains the use of Cu ionophores to increase the Cu content and induce apoptosis of cancer cells. The anti-cancer effects of Cu ionophores have been demonstrated in several studies.[17] Inhibition of inflammatory breast cancer by disulfiram was confirmed in both in vitro and in vivo experiments,[22] and the synergistic effects of disulfiram and docosahexaenoic acid effectively inhibited the tumor growth and promoted the apoptosis of cancer cells.[23] The cytotoxic mechanisms of metal ions, including Cu, are suggested to mainly rely on oxidative stress.[24] Oxidative stress is caused by an increase in the levels of reactive oxygen species or highly toxic hydroxyl radicals beyond the antioxidant capacity of the cell.[25] However, a recent study published in *Science* challenges this conventional view.[26] That study revealed that intracellular Cu accumulation can induce a novel regulatory cell death mechanism via the aggregation of lipoylated mitochondrial enzymes and the destabilization of the Fe–S cluster proteins, which is termed as "cuproptosis."[26,27] This unique type of cell death is not affected by the levels of reactive oxygen species and is different from all other oxidative stress-related cell death mechanisms, including ferroptosis. [26,27] Importantly, that study also found that tumor cells dependent on galactose-mediated mitochondrial respiration were nearly 1 000-fold more sensitive to cuproptosis than cells dependent on glucose-induced glycolysis.[26,27] Given that glycolysis is critical for tumor cell growth and metabolism, inhibition of glycolysis would not only suppress tumor malignancy, but also enhance sensitivity to cuproptosis, implying that the regulation of cuproptosis in tumor cells may be synergistic with other therapeutic modalities and can be potentially used to develop novel therapeutic strategies.[27] In addition, to identify the genes involved in cuproptosis, the authors performed a genome-wide CRISPR-Cas9 loss-of-function screening and identified 10 cuproptosis regulators. Among them, seven cuproptosis regulators were found to be involved in the positive regulation of cuproptosis, namely ferredoxin 1 (FDX1), lipoyl synthase (LIAS), lipolytransferase 1 (LIPT1), dihydrolipoamide dehydrogenase (DLD), dihydrolipoamide S-acetyltransferase (DLAT), pyruvate dehydrogenase E1 subunit alpha 1, and pyruvate dehydrogenase E1 subunit beta.[26] Meanwhile, three of them were found to be involved in the negative regulation of cuproptosis, namely the metal regulatory transcription factor 1 (MTF1), glutaminase (GLS), and cyclin-dependent kinase inhibitor 2A (CDKN2A).[26] The identification of these cuproptosis regulators facilitated the subsequent exploration of the mechanisms underlying Cu toxicity and regulation of this new type of cell death.

New cell death mechanisms often lead to the identification of novel tumor therapeutic targets and development of personalized treatment strategies for patients. For example, cells that undergo mitochondrial respiration and those with high levels of lipoylated proteins are highly sensitive to cuproptosis, indicating that Cu ionophore therapy may be very effective for tumors with this metabolic profile.[26] It is conceivable that a great deal of future research will focus on the potential impact of cuproptosis on tumor development and how this unique death mechanism can be exploited to improve

the prognosis of patients with cancer and to benefit the larger biomedical community. To provide an initial overview and reference point for future studies, we used big data to comprehensively assess the molecular and clinical characteristics of cuproptosis regulators in 33 tumors from a multi-omics perspective. Our study showed that cuproptosis is closely related to the prognosis of multiple tumors, activation/inhibition of cancer hallmark pathways, and regulation of the tumor microenvironment. Rational use of cuproptosis exhibits great potential for future cancer therapies.

Results

Somatic alteration landscape of cuproptosis regulators

To understand the genomic alterations in the 10 cuproptosis regulators in tumors, we analyzed the single nucleotide variation (SNV) and copy number variation (CNV) data from 10 680 pan-cancer samples to calculate the mutation frequencies and somatic copy number alterations (SCNA). Somatic alterations were defined as mutations or SCNA. Overall, the frequency of somatic alterations was very low for all cuproptosis regulators (1–3%), except CDKN2A that showed somatic alterations in up to 18% of the tumors (Fig. 1A). Most somatic alterations in CDKN2A were deep deletions (Fig. 1A). We characterized the somatic alterations in these cuproptosis regulators in each of the 33 tumors to better understand the landscape of the different tumor types. Different tumor types had different mutation patterns, and all 10 cuproptosis regulators exhibited mutations in bladder urothelial carcinoma (BLCA), colon adenocarcinoma (COAD), head and neck squamous cell carcinoma (HNSC), and uterine corpus endometrial carcinoma (UCEC), whereas no mutations were observed in diffuse large B-cell lymphoma, kidney chromophobe, testicular germ cell tumors, and uveal melanoma (UVM) (Fig. 1B). In addition, the highest mutation frequencies of CNKN2A were observed in HNSC (19.3%) and pancreatic adenocarcinoma (19.1%). For amplification, all cuproptosis regulators in BLCA, lung adenocarcinoma (LUAD), ovarian serous cystadenocarcinoma, and UCEC were amplified, whereas all those in UVM remained unchanged (Fig. 1C). DLD in esophageal carcinoma had the highest amplification frequency (8.5%). Consistent with Fig. 1A, a high percentage of CDKN2A deep deletion was observed in most tumor types (Fig. 1D). Among them, more than half of the glioblastoma multiforme samples showed deep deletion of CDKN2A, while UVM only showed a low percentage of deletions in FDX1 (1.3%) and DLAT (1.3%). Overall, cuproptosis regulators show a heterogeneous pattern of somatic alterations in different tumor types. Given that gene amplification and deep deletion largely mediate aberrant gene expression,[28] we explored the effects of amplification and deep deletion on cuproptosis regulator expression in cancer. Consistent with expectations, amplification samples had the highest gene expression and deep deletion samples had the lowest gene expression among all 10 cuproptosis regulators (Supplementary information, Fig. S1). This suggests that SCNA affects the expression levels of cuproptosis regulators in tumors.

Gene expression patterns of cuproptosis regulators

To characterize the gene expression patterns of cuproptosis regulators, we first explored the interaction relationships among the regulators using the STRING database. As shown in Supplementary information, Fig. S2, the seven positive regulators and the negative regulator, GLS, formed an interaction network, whereas MTF1 and CDKN2A did not interact with other regulators. We further explored the distribution of regulator expression in different normal tissues. Overall, the expression of the regulators was evenly distributed in different tissues, with the highest expression of FDX1 in the adrenal gland and very low expression of CDKN2A in the bone marrow (Supplementary information, Fig. S3).

Differential expression analysis of paired normal and tumor tissues revealed that cuproptosis regulators were aberrantly expressed in 17 tumors (Fig. 2A). FDX1 expression was downregulated in 12 tumors, LIPT1 expression was downregulated in eight tumors, and CDKN2A expression was significantly upregulated in 16 tumors. Other regulators showed heterogeneous expression patterns; for example, LIAS expression was downregulated in most tumors, whereas its expression was increased in kidney chromophobe and LUAD. Subsequently, we explored the role of co-expression of the regulators in 33 tumors. The expression correlations prevalent among all regulators in all tumor types are shown in Supplementary information, Table S1. FDX1 expression was significantly positively correlated with the expression levels of six other positive regulators in most tumors. This suggests that cuproptosis regulators in tumors may co-regulate their cuproptosis activity.

To better understand the expression landscape of cuproptosis regulators in tumors, we performed unsupervised consensus clustering based on regulator mRNA expression for all samples of the 33 tumor types. Based on the consensus cumulative distribution function and delta area, all tumors were distinctly divided into two different sample clusters (Fig. 2B). Compared to cluster 2, cluster 1 had higher expression levels of FDX1, LIAS, LIPT1, DLD, DLAT, pyruvate dehydrogenase E1 subunit beta, and GLS, and significantly lower expression levels of CDKN2A (Fig. 2C). Examination of the distribution of all cancer types in the two clusters revealed that all acute myeloid leukemia, most COAD, three types of kidney cancers (kidney chromophobe, kidney renal clear cell carcinoma [KIRC], and kidney renal papillary cell carcinoma [KIRP]), prostate adenocarcinoma, rectum adenocarcinoma, testicular germ cell tumors, and thyroid carcinoma (THCA) were distributed in cluster 1, and most of the three types of gynecologic tumors (cervical squamous cell carcinoma and endocervical adenocarcinoma, ovarian serous cystadenocarcinoma, and uterine carcinosarcoma) were distributed in cluster 2 (Fig. 2D). As cuproptosis in tumors is regulated by 10 regulators, the expression of any individual regulator can hardly reflect the overall level of cuproptosis. Therefore, according to previous research methodology,[29-31] we first proposed the cuproptosis positive score, cuproptosis negative score, and cuproptosis activity score based on the mRNA expression levels of positive and negative regulators of cuproptosis. In the pan-cancer context, the positive cuproptosis score was positively correlated with the expression of all positive regulators, and the negative cuproptosis score was positively correlated with the expression of all

negative regulators (Supplementary information, Fig. S4). The cuproptosis activity score was positively correlated with the cuproptosis positive score as well as positive regulator expression and negatively correlated with the cuproptosis negative score as well as negative regulator expression (Supplementary information, Fig. S4); thus, the cuproptosis activity score integrated the expression abundance of all regulators and better reflected the overall cuproptosis level. Subsequently, we found that cluster 1 had significantly higher cuproptosis positive and activity scores, and lower negative scores than cluster 2 (Fig. 2E), suggesting that cluster 1 had a relatively higher level of cuproptosis. Survival analysis showed that cluster 1 had a significantly better overall prognosis than cluster 2 (Fig. 2F), implying that the cuproptosis level may influence the survival of patients with different tumor types.

Methylation analysis of cuproptosis regulators

Methylation in the promoter regions of genes largely regulates the gene expression, and hypermethylation generally suppresses the gene expression.[32] However, there are some special cases where hypermethylation of the promoter region may enhance the expression of a gene, such as human telomerase reverse transcriptase.[33] To explore the methylation alterations in cuproptosis regulators, we first compared the methylation differences in the regulators between paired normal and tumor tissues. As shown in Fig. 3A, the methylation levels of regulators varied in all 16 tumors. Methylation alterations in regulators were heterogeneous in different tumor types. For example, the methylation levels of FDX1 were elevated in BLCA, BRCA, COAD, HNSC, KIRP, and UCEC tumor tissues compared to paired normal tissues, while they were decreased in KIRC. Notably, MTF1 did not show altered methylation levels in any of the tumor types. Furthermore, we analyzed the correlation between regulatory methylation levels and mRNA expression levels in 33 tumor types. In most tumor types, the promoter methylation levels of FDX1, DLAT, GLS, and CDKN2A were negatively correlated with the mRNA expression levels (Fig. 3B). The methylation levels of LIAS, DLD, pyruvate dehydrogenase E1 subunit alpha 1, pyruvate dehydrogenase E1 subunit beta, and MTF1 were negatively or positively correlated with the mRNA expression levels in specific tumor types. For example, MTF1 was negatively correlated with BRCA, cervical squamous cell carcinoma and endocervical adenocarcinoma, DLBC, and brain low-grade glioma (LGG) and positively correlated with THCA (Fig. 3B). Notably, the methylation levels of LIPT1 were positively correlated to the mRNA expression levels in most tumor types. Survival analysis revealed that the methylation levels of cuproptosis regulators were correlated with the overall survival (OS) in 17 tumor types and that the correlations were tumor type-dependent. For instance, FDX1 hypermethylation was associated with poor OS in LGG and good OS in UVM (Fig. 3D, E).

MicroRNAs (miRNAs), long non-coding RNAs (lncRNAs), and transcription factors (TFs) regulate the expression levels of cuproptosis regulators

In previous results of this study, we described the regulation of cuproptosis regulators expression by SCNA and DNA methylation. miRNAs are gene expression repressors that can regulate gene expression post-transcriptionally by binding to the 3'-untranslated regions of target mRNAs.[34,35] To comprehensively explore miRNAs that may regulate cuproptosis regulators, we screened all miRNAs that could target the 3'-untranslated regions of these regulators. In Supplementary information, Table S2, we have listed all potential miRNA–mRNA pairs that may target different cuproptosis regulators in each tumor type after threshold screening as a reference for future cuproptosis-related miRNA studies. Notably, 174 miRNA–mRNA pairs, including 127 miRNAs, were present in at least five tumor types. Interestingly, 33 of the 127 miRNAs targeted at least two cuproptosis regulators, constituting a miRNA regulatory network (Fig. 4A). Given that these miRNAs target multiple regulators in multiple tumors, these miRNAs may be potential miRNAs regulating cuproptosis.

LncRNAs are important regulators of gene expression and play important roles in transcription, translation and post-translational modifications.[36] Therefore, we combined lncRNA regulation pan-cancer analysis with gene expression correlation analysis data to filter all potential lncRNA–mRNA pairs regulating cuproptosis in different tumor types (Supplementary information, Table S3).[37] A total of 131 lncRNA–mRNA pairs were identified involving 55 lncRNAs, 34 of which targeted at least two cuproptosis regulators and constituted an lncRNA regulatory network (Fig. 4B).

TFs are key regulators of gene transcription and expression, and dysregulated TFs mediate aberrant gene expression and represent a unique class of drug targets.[38] We examined a series of TFs listed in a previous pan-cancer study and identified a total of 465 TF–mRNA pairs containing 208 different TFs,[37] of which 24 TFs regulated the expression levels of at least five cuproptosis regulators (Fig. 4C). Importantly, nuclear factor I C (NFIC) targeted all 10 cuproptosis regulators, suggesting that it may be a key TF mediating cuproptosis in tumors. Supplementary information, Table S4 lists all TF–mRNA pairs that may target cuproptosis regulators in different tumor types.

Cuproptosis activity predicts the prognosis of patients with cancer

The results of this study demonstrated that cuproptosis activity predicted the OS in a pan-cancer context. To further clarify the impact of cuproptosis on patient survival, we explored the prognostic predictive roles of cuproptosis regulators and cuproptosis scores for different tumor types. We performed Cox regression analysis on cuproptosis regulators or scores to calculate the survival risk and used the log-rank test to determine significance after dividing different tumors into two groups according to the median of cuproptosis regulators or scores. As shown in Fig. 5A, cuproptosis regulators and scores had different prognostic roles in different tumor types. High LIAS expression was associated with better OS in

adrenocortical carcinoma, COAD, KIRC, KIRP, LGG, liver hepatocellular carcinoma (LIHC), and mesothelioma, while high CDKN2A expression was associated with poor OS in adrenocortical carcinoma, COAD, KIRC, LIHC, pheochromocytoma and paraganglioma, prostate adenocarcinoma, UCEC, and UVM. In addition, an elevated cuproptosis activity score was associated with poorer OS in HNSC and better OS in patients with KIRP, LIHC, and UCEC. Fig. 5B and C show the Kaplan–Meier survival curves between the high and low cuproptosis activity score groups after dividing the samples into two groups according to the median value in HNSC and UCEC, respectively. To further confirm the effect of cuproptosis on the OS of patients, we performed Kaplan–Meier survival curve analysis after dividing the patients into two groups according to the best cut-off value of the cuproptosis activity score. The results showed that the cuproptosis activity was significantly associated with the OS in 13 of the 33 tumor types (Supplementary information, Fig. S5). Among them, higher cuproptosis activity predicted better OS in COAD, diffuse large B-cell lymphoma, KIRP, acute myeloid leukemia, LGG, LIHC, lung squamous cell carcinoma, sarcoma, and UCEC and also predicted poorer OS in HNSC, LUAD, skin cutaneous melanoma, and UVM. In addition to OS, we also tested the relationship between cuproptosis and disease-free interval and progression-free interval in patients with tumors. We found that the cuproptosis regulator levels and activity scores were strongly correlated with disease-free interval in 16 tumor types and progression-free interval in 20 tumor types, with the correlation depending on the tumor type. These results suggest that cuproptosis is correlated with the prognosis of specific tumor types and can predict patient survival.

Pathway activity analyses of cuproptosis

Our results demonstrated the dysregulation and prognostic role of cuproptosis in tumors; however, the specific tumor-related pathways involved in cuproptosis remain unknown. Therefore, we first inferred the enrichment level of 50 cancer hallmark gene sets in all tumor samples from 33 tumor types (Supplementary information, Table S5), which comprehensively reflected the biological processes associated with tumors.[39] Subsequently, we calculated the correlation of the cuproptosis activity score with all hallmark gene sets in each tumor type and generated a heatmap (Fig. 6A; Supplementary information, Table S6). Cuproptosis activity was positively correlated with approximately half of the hallmark gene sets in most tumor types and negatively correlated with the other half, indicating that cuproptosis plays a key role in tumors (Fig. 6A). Notably, cuproptosis activity was significantly positively correlated with oxidative phosphorylation in all 33 tumor types (Fig. 6B), which is consistent with the study by Tsvetkov et al. that cuproptosis is dependent on mitochondrial respiration and the tricarboxylic acid (TCA) cycle,[26] further suggesting that the cuproptosis activity score can reliably reflect the cuproptosis level. In addition, cuproptosis was also significantly negatively correlated with hypoxia in 24 tumor types (Fig. 6B), and Tsvetkov et al. found that hypoxia (1% O_2) reduces cuproptosis sensitivity by obliging cells to rely on glycolysis rather than oxidative phosphorylation.[26,27] Cuproptosis was also significantly positively correlated to fatty acid metabolism in all tumor types (Fig. 6B). Additionally, cuproptosis was negatively associated with the apical junction, mitotic spindle, epithelial–mesenchymal transition (EMT), transforming growth factor (TGF)-β, KRAS, and tumor necrosis factor-alpha signaling

pathways in more than 25 cancer types, confirming the important regulatory role of cuproptosis in tumor metastasis and growth. Strikingly, cuproptosis was also negatively associated with immune-related pathways, including the inflammatory response, complement, interleukin-6/Janus kinase/signal transducer and activator of transcription 3 signaling, and interferon gamma response pathways, in most tumor types (Fig. 6B). Given that cuproptosis was positively associated with DNA repair in 27 tumor types, we further explored whether cuproptosis was related to genomic instability. Consistent with expectations, cuproptosis was negatively associated with the indicators related to homologous recombination deficiency (HRD) in 11 tumor types, but negatively associated with mutational burden in only three tumor types (Supplementary information, Fig. S6). In summary, the above results suggest that cuproptosis is involved in numerous biological processes in tumors.

Cuproptosis-associated immune characteristics

In pathway activity analyses, we observed significant correlations between cuproptosis and immune-related pathways. To better reveal the intrinsic link between cuproptosis and tumor immunity, we first inferred the overall immune (ImmuneScore) and stromal (StromalScore) infiltration levels in all tumor samples (Supplementary information, Table S7). Consistent with the results of the pathway activity analyses, cuproptosis was significantly negatively correlated with the overall immune and stromal cell infiltration levels in most tumor types (Fig. 7A). In addition, cuproptosis was negatively correlated with the ESTIMATEScore of tumors, indicating that cuproptosis is positively correlated with tumor purity. To further understand the correlation between cuproptosis and the abundance of different types of immune cells, we collected the infiltration levels of 22 immune cells of all tumor samples from a previous pan-cancer analysis.[40] We calculated the correlation between cuproptosis and the levels of immune cell infiltration in each tumor type (Supplementary information, Table S8). As shown in Fig. 7B, there was a heterogeneous correlation pattern between cuproptosis and tumor-infiltrating immune cells. In 11 tumor types, cuproptosis was negatively correlated with the abundance of M1 macrophages, whereas in 10 tumor types, cuproptosis was positively correlated with the abundance of follicular helper T cells (Fig. 7C). Overall, cuproptosis was correlated with the abundance of numerous immune cells, and the correlation may vary depending on the tumor type. Immunomodulators are crucial for the response to immunotherapy, and we collected some classical immune activation-related genes, immune checkpoint-related genes, and TGFβ/EMT pathway-related genes from a previous study by Zeng et al.[41] We then calculated the correlation between cuproptosis and these immunomodulators (Supplementary information, Table S9). In general, cuproptosis was negatively correlated with most immunomodulators in most tumor types, which is consistent with the results of previous studies (Fig. 7D). Although immune activation-related genes appear to be positively associated with cuproptosis in some specific tumor types, such as glioblastoma multiforme, this correlation was not significant (Supplementary information, Table S9). Thorsson et al. classified all samples from 33 tumor types into six immune subtypes (C1-C6) with different immune characteristics in a pan-cancer context and were widely recognized,[40] Therefore, we compared the differences in cuproptosis between the six immune subtypes. As shown in Fig. 7E, C4

(lymphocyte depleted) tumors had the highest level of cuproptosis activity, whereas C6 (TGF-β-dominant) tumors had the lowest cuproptosis activity. This further validated the negative correlation between cuproptosis and the TGF-β pathway. Based on this result, we can hypothesize that the lower immune response in high cuproptosis tumors may be related to lymphocyte depletion. These results imply a broad link between cuproptosis and tumor immunity.

Association of cuproptosis with drug sensitivity and immunotherapy outcome

After establishing the association of cuproptosis with numerous cancer hallmark pathways and immune-related characteristics, we aimed to understand whether cuproptosis could influence patient response to chemotherapy, targeted therapies, and immunotherapy. We integrated gene expression data and drug sensitivity data of cancer cell lines from the Genomics of Drug Sensitivity in Cancer database and analyzed the correlation of cuproptosis with the half maximal inhibitory concentration (IC_{50}) of 198 drugs. Unexpectedly, we observed significant negative correlations between cuproptosis and the IC_{50} of 39 drugs but failed to observe a positive correlation between cuproptosis and the IC_{50} of any drug (Fig. 8A), suggesting that cuproptosis broadly increases the sensitivity of chemotherapy and targeted drugs. By examining the mechanism of action of these 39 drugs, it was found that some of the targeted pathways had been shown to be negatively associated with cuproptosis activity in the previous results. For example, cuproptosis in the pathway activity analyses was negatively correlated with the P53 and PI3K/MTOR pathways in 13 tumor types (Fig. 6B), and cuproptosis was associated with increased sensitivity to two P53 pathway inhibitors (MIRA-1 and Nutlin-3a (-)) and three PI3K/MTOR pathway inhibitors (Ipatasertib, LJI308, and Uprosertib) (Fig. 8A), which further enhanced the reliability of our study. Generally, a high cuproptosis activity indicates higher chemotherapy and targeted drug sensitivity.

Immune checkpoint inhibitor (ICI) therapy is currently the most successful and common immunotherapy approach.[42,43] To further investigate whether cuproptosis affects ICI therapy outcomes in tumor patients, we collected a metastatic urothelial cancer cohort receiving anti-programmed death ligand-1 (PD-L1) therapy (IMvigor210) and a metastatic melanoma cohort receiving anti-programmed death-1 (PD-1) therapy (GSE78220) from previous studies.[30,44] In the IMvigor210 cohort, cuproptosis was found to be negatively correlated with the tumor ImmuneScore, StromalScore, and ESIMATEScore (Fig. 8B). More importantly, cuproptosis was negatively correlated with PD-L1 expression in this cohort (Fig. 8C). Interestingly, Kaplan-Meier survival curve analysis showed that patients with high cuproptosis activity had longer survival after anti-PD-L1 therapy than those with low cuproptosis activity (Fig. 8D). In the GSE78220 cohort, although cuproptosis did not correlate with PD-1 expression (Fig. 8E), Kaplan–Meier survival curve analysis demonstrated that patients with high cuproptosis activity had a better OS after

anti-PD-1 treatment than those with low cuproptosis activity (Fig. 8F). These results provide preliminary evidence of the predictive role of cuproptosis in ICI immunotherapy.

Discussion

Cu acts as a double-edged sword, and imbalance in its homeostasis can seriously endanger the human life.[45–47] Both Cu chelators and Cu ionophores act as promising anti-cancer agents.[17,19,20,48–50] Previous studies suggested that the mechanism of Cu overload toxicity depends on oxidative stress.[1,27] However, Tsvetkov et al. first revealed cuproptosis, a completely new form of cell death different from the previously known regulated cell death and screened 10 regulators of cuproptosis.[26] Unlike oxidative stress-dependent regulated cell death processes, such as apoptosis and ferroptosis, cuproptosis is dependent on mitochondrial stress and is induced by Cu binding to lipoylated components of the TCA cycle.[26] As a new and completely different form of regulated cell death that has never been characterized before, cuproptosis-based tumor research is expected to flourish. Therefore, preliminary studies on the role of cuproptosis in tumors are necessary to further understand the mechanisms of tumor development and explore new clinical therapies. This study provides a comprehensive and integrated characterization of cuproptosis by mining and analyzing multi-omics data from more than 10 000 samples of 33 tumor types from The Cancer Genome Atlas (TCGA).

Genetic variation analysis revealed that most cuproptosis regulators had a low proportion of somatic alterations in tumors; however, CDKN2A underwent extensive somatic alterations in a variety of tumors. This is consistent with the currently available knowledge that CDKN2A is involved in cell growth and cycle regulation,[51,52] and that its mutation and loss are important events in many tumors and contribute to multiple tumorigenesis.[53,54] However, we found that the mRNA expression of CDKN2A, a tumor suppressor, was significantly upregulated in 16 tumor types. Although deletion of CDKN2A could reduce its expression, CDKN2A showed hypomethylation in BRCA, esophageal carcinoma, HNSC, LIHC, and lung squamous cell carcinoma, suggesting that CDKN2A upregulation in these tumors may be mainly regulated by hypomethylation. Interestingly, CDKN2A expression and methylation levels were elevated in both KIRP and THCA, yet CDKN2A hypermethylation in both tumors upregulated gene expression, suggesting that high CDKN2A expression in KIRP and THCA is also regulated by hypermethylation. This anomaly suggests tumor type-dependent regulation of gene expression by methylation of CDKN2A and warrants further investigation. For some specific tumors, such as lung squamous cell carcinoma, the expression of CDKN2A was significantly elevated despite the presence of substantial deep deletion and hypermethylation, indicating that CDKN2A expression was mainly influenced by other mechanisms in these tumors, such as miRNAs, lncRNAs, and TFs. Furthermore, although the oncogenic effects of mutations and loss of CDKN2A are well established,[55] unexpectedly high CDKN2A expression indicates a poor prognosis in a variety of tumors. Similarly, previous studies have shown that high CDKN2A expression is associated with poor prognosis in LIHC, COAD, and BLCA.[56–59] However, the mechanism by which CDKN2A acts as a tumor suppressor but leads to poor prognosis has not been clarified. Shi et al. speculated that this might be related to the involvement of CDKN2A in the EMT process.[58] Since the role

of CDKN2A as a negative regulator of cuproptosis has never been characterized before. Considering that high cuproptosis activity was revealed to be a favorable prognostic factor in multiple tumors (including COAD and LIHC) in the present study, it is reasonable to assume that CDKN2A may contribute to the poor prognosis of these tumors by negatively regulating cuproptosis activity, which is worthy of in-depth study in the future to develop suitable targeted agents.

High expression of FDX1, the most important positive regulator of cuproptosis, was only associated with a favorable prognosis in COAD and LIHC, which may be due to the upregulation of cuproptosis activity by FDX1. However, FDX1 did not correlate with the prognosis of most tumor types, consistent with the study by Zhang et al. who also showed that FDX1 was unable to affect proliferation and apoptosis of LUAD cells.[60] Considering the prognostic impact of cuproptosis activity on many tumor types, it is necessary to consider all cuproptosis regulators as a whole. Accordingly, we developed the cuproptosis activity score, and correlation and pathway activity analyses adequately demonstrated that cuproptosis activity scores can reflect the overall cuproptosis level, which provides a reference method for future cuproptosis studies.

The regulatory roles of miRNAs, lncRNAs, and TFs in gene expression are well known;[34,36,38] There is no doubt that there must be miRNAs, lncRNAs and TFs that can indirectly regulate cuproptosis. To pave the way for further related studies, we identified potential cuproptosis-related miRNAs, lncRNAs, and TFs, and constructed regulatory networks. Among the identified miRNAs, some have been verified in previous studies, such as miR-10b targeting CDKN2A in gliomas,[61] which further supports the reliability of our study. Interestingly and importantly, there were some interactions between the potential miRNA–mRNA pairs and lncRNA-mRNA pairs that we identified. For example, both lncRNA MEG3 and miR-204 in this study could target CDKN2A, and in a previous study MEG3 was found to regulate inflammation and apoptosis in macrophages via the MEG3/miR-204/CDKN2A regulatory axis.[62] This suggests that the lncRNAs identified in this study may also regulate cuproptosis regulator expression via miRNAs in the mechanism of competing endogenous RNA.[63] Therefore, it seems feasible and promising to combine the lncRNAs and miRNAs we identified for further study. It is important to mention that the TF NFIC targets all 10 cuproptosis regulators in the regulatory network, implying that NFIC may be a key upstream TF of cuproptosis. The role of NFIC in the regulation of growth and metastasis of a variety of tumors has been confirmed, and its mechanism involves the EMT process and NF-κB pathway.[65–69] However, the association of NFIC with cuproptosis activity has never been characterized; therefore, we hypothesized that NFIC could also affect tumor development by regulating cuproptosis activity, which deserves further exploration.

In the pathway activity analyses, we noted strong correlations among cuproptosis, oxidative phosphorylation, and hypoxia, which stem from the mechanism of cuproptosis occurrence that has been elucidated in detail by Tsvetkov et al.[26] Moreover, we revealed a negative correlation between cuproptosis and multiple tumor-related pathways, which directly provides a theoretical basis for our findings in the drug sensitivity analysis. Notably, in our results, high cuproptosis activity was not only associated with high sensitivity to multiple drugs but also did not increase resistance to any chemotherapy or targeted

drugs, implying that Cu ionophores have the potential to synergize with multiple drugs as broad-spectrum anti-tumor agents. This finding has been validated in previous experiments. For example, drug sensitivity analysis showed that cuproptosis increased the sensitivity of three PI3K inhibitors, while in the study by Zhang et al., the combination of the Cu ionophore disulfiram with PI3K inhibitors significantly inhibited breast cancer growth in both ex vivo and in vitro experiments.[70] In addition to its relevance to tumor-related pathways, another finding of interest was that cuproptosis was positively correlated with fatty acid metabolism in all tumor types. Tsvetkov et al. only reported that cuproptosis was more sensitive in cells dependent on mitochondrial respiration (oxidative phosphorylation) but did not mention fatty acid metabolism. Fatty acid metabolism is an important component of cancer cell metabolism. In fatty acid metabolism, β-oxidation breaks down the long carbon chains of fatty acids into acetyl-CoA and then sends them to the TCA cycle.[71,72] These processes take place in the mitochondria. Given that cuproptosis is dependent on mitochondrial stress and the binding of Cu to lipoylated components of the TCA cycle,[26,27] combined with our results, it is reasonable to believe that tumors with high fatty acid metabolism are equally sensitive to cuproptosis. This may contribute to the development of individualized cuproptosis therapy.

Strikingly, the present study revealed a strong correlation between cuproptosis and immune-related pathways and signatures in most tumors, suggesting that cuproptosis may be involved in tumor microenvironment remodeling in tumors. High cuproptosis activity tends to imply lower immune response and immune cell infiltration. As existing studies have shown that oxidative phosphorylation and TCA cycle metabolism are also crucial in immune cell activation and metabolism, we consider that immune cells may be equally sensitive to cuproptosis. Although previous studies have shown that pre-existing anti-tumor immunity tends to be associated with a better prognosis,[74] however, in our study, although high cuproptosis activity reduced the immune response, it still improved the prognosis of a variety of tumors. This may seem contradictory; however, numerous studies have also shown that even a large immune component does not mean a better prognosis, which is related to various factors, such as the aggressiveness of the tumor itself, the composition of the tumor microenvironment, and the relative predominance of immune stimulatory and suppressive factors.[40,44,75,76] Thus, the better prognosis in high cuproptosis tumors may be associated with low stromal infiltration and low immunosuppression. This may also be one of the reasons why patients with high cuproptosis in the immunotherapy cohort had better outcomes. In the immunotherapy cohorts, although cuproptosis activity was negatively or not correlated with immune infiltration and PD-(L)1 expression, patients with high cuproptosis still had good outcomes, possibly due to the lower stromal infiltration. In fact, PD-(L)1 expression in recent studies has failed to serve as a good predictor of response to ICI therapy.[44,77] Furthermore, clinical trial-based studies have demonstrated that TGF-β attenuates tumor response to anti-PD-L1 therapy by excluding T cells.[44] The present study revealed that in patients with high cuproptosis activity, low TGF-β signaling may account for the positive outcome of patients with high cuproptosis in ICI therapy. However, the specific effects and mechanisms of cuproptosis in immunotherapy need to be elucidated in future basic and clinical studies.

In conclusion, this study is the first to comprehensively examine the clinical and molecular characteristics of cuproptosis regulators and cuproptosis activity in 33 tumors, providing valuable resources and a reference point for future cuproptosis-related studies. We showed that cuproptosis is associated with multiple tumour-related pathways and immune signatures; therefore, it may be used to develop a novel strategy for the treatment of cancer.

Materials And Methods

SNV and CNV analysis

SNV and CNV data of 33 tumor types (n = 10 680) from TCGA database were obtained from the cBioPortal (https://www.cbioportal.org/). SNV data retained only non-silent mutations, including Missense_Mutation, Nonsense_Mutation, Frame_Shift_Del, Splice_Site, Frame_Shift_Ins, In_Frame_Del, and Nonstop_Mutation in this study. According to previous studies,[40] values equal to 2 in CNV data are considered as amplifications and values equal to –2 are considered as deep deletions. SNV and CNV ratios were calculated for each tumor type. In addition, the overall somatic alterations in the OncoPrint plot were generated using the R package “ComplexHeatmap”.

mRNA expression analysis and cuproptosis scores

Normal tissue expression data from the Genotype-Tissue Expression dataset were obtained from the Xena Functional Genomics Explorer (https://xenabrowser.net/datapages/) to compare the expression differences of cuproptosis regulators in different normal tissues of healthy individuals, containing a total of 7 823 samples from 28 different tissues. In addition, gene expression data and clinical information for 11 060 tumor patient samples from the TCGA dataset were also obtained from Xena. The gene expression data were normalized, the batch effect was corrected, and the expression data were log2(x+1) transformed. The interaction network between the cuproptosis regulators was constructed using the STRING database (https://string-db.org/). Of the 33 tumor types, only 17 tumor types containing more than five pairs of tumor and normal samples were included in the differential expression analysis between tumor and normal samples. The fold change was calculated as the ratio of the mean of the tumor sample expression to the mean of the normal sample expression, and the p-value was obtained using the t-test. Based on the mRNA expression levels of cuproptosis regulators, potential cuproptosis-related clusters were identified via unsupervised consensus clustering based on the PAM algorithm. A total of 1 000 bootstrap runs were performed, with each bootstrap including 80% of the patients and the number of clusters set to 2–10. The consensus cumulative distribution function and delta area were used to define the optimal number of clusters.[78]

To understand the overall cuproptosis level of each sample, we used a previously reported method. [29-31,79] The GSVA algorithm was used to calculate the gene set enrichment scores for positive and negative regulators of cuproptosis, which were defined as the cuproptosis positive score and cuproptosis negative score, respectively, and the cuproptosis activity score was defined as the difference between them.

Methylation analysis

DNA methylation data for TCGA samples (Methylation450K, n = 9 639) were obtained from Xena, and only those probes that mapped to the promoter region of the cuproptosis regulator were used for subsequent analysis. For genes containing multiple probes, the mean β value of all probes was used as the methylation level. Only 16 tumor types with at least five tumor–normal pairs were retained in the differential methylation analysis, and fold change and p-values were calculated using the same method as that used for differential expression analysis. Subsequently, after integrating the methylation and gene expression data of cuproptosis regulators, correlations and p-values were determined using Spearman's correlation analysis.

After combining the methylation data of cuproptosis regulators and clinical information, the hazard ratio of regulator methylation was calculated based on Cox regression analysis. Hazard ratio > 1 represented high methylation associated with poor OS, which indicates a high risk. Each tumor type was divided into two groups based on the median methylation level of each regulator and a log-rank test was performed to calculate the p-value.

miRNA, lncRNA, and TF analyses

The normalized miRNA expression data of TCGA samples (n = 10 818) were downloaded from Xena, and the batch effect was corrected. The miRNA regulatory data of cuproptosis regulators were collected from databases, including experimentally validated (miRTarBase v9.0 and TarBase v8.0) and predicted (Targetscan v8.0) miRNA–mRNA pairs. Subsequently, miRNA and mRNA expression data from TCGA were integrated, and for each tumor type, correlations were calculated separately for each miRNA–mRNA pair using Spearman's correlation analysis. Only miRNA–mRNA pairs with correlation coefficients < -0.2 and $P < 0.05$ were considered as potential regulatory pairs. The miRNA regulatory network was constructed using Cytoscape_v3.8.2.

The lncRNA and TF regulatory data were obtained from a previous pan-cancer study.[37] Using this data, we screened potential lncRNA–mRNA pairs and TF–mRNA pairs targeting cuproptosis regulators in each

tumor and calculated the expression correlation of each lncRNA–mRNA and TF–mRNA pair using Spearman's correlation analysis for each tumor type. Only lncRNA–mRNA pairs with absolute values of correlation coefficients > 0.1 and P < 0.05, and TF–mRNA pairs with absolute values of correlation coefficients > 0.2 and P < 0.05, were retained. The lncRNA and TF regulatory networks were constructed using Cytoscape_v3.8.2.

Survival analysis

After integration of cuproptosis regulator expression data, cuproptosis scores, and clinical information, samples without survival information were excluded. Hazard ratios were calculated for each variable relative to OS, disease-free interval, and progression-free interval for each tumor type based on Cox regression analysis to determine high or low risk. Each tumor was divided into two groups using the median of each variable as the cutoff value, and a log-rank test was performed to determine the P-values. For OS, we also calculated the optimal cutoff value of cuproptosis activity score in each tumor using the R package "maxstat" and used optimal cutoff value to divide the tumors into two groups to plot the Kaplan–Meier survival curves and perform log-rank tests.

Pathway activity analyses

The cancer hallmark gene sets (h.all.v7.5.1.symbols.gmt) were downloaded from the Molecular Signatures Database (https://www.gsea-msigdb.org/gsea/msigdb/), and the GVSA algorithm was used to infer the hallmark pathway scores for all tumor samples in TCGA. The correlation between the cuproptosis activity score and each hallmark pathway was subsequently calculated for each tumor type using Spearman's correlation analysis. In addition, the mutation burden, HRD score, loss of heterozygosity (LOH) score, large-scale state transitions (LST) score, and telomeric allelic imbalance (TAI) score were collected from a previous study.[80] HRD score was the sum of LOH, LST, and TAI scores.

Immune characteristic analysis

The ImmuneScore (representing the overall level of immune cell infiltration), StromalScore (representing the overall level of stromal infiltration), and ESTIMATEScore (negatively correlated with tumor purity) were inferred for each tumor sample using the ESTIMATE algorithm,[81] and the correlation between the cuproptosis activity score and these three were calculated for each tumor type using Spearman's correlation analysis. The abundance of 22 immune cells calculated based on the CIBERSORT algorithm was collected from a previous publication, and the correlation between immune cell abundance and cuproptosis activity was calculated for each tumor type.[40] In addition, immune activation-related

genes, immune checkpoint-related genes, and TGFβ/EMT pathway-related genes were collected from a previous publication by Zeng et al.[41]

For the immunotherapy datasets, gene expression data and clinical information for the IMvigor210 cohort were obtained from IMvigor210 Core Biologies (http://research-pub.gene.com/IMvigor210CoreBiologies).[44] Gene expression data were converted to transcripts per kilobase million values and log2(x +1) transformation was performed. Normalized gene expression data and clinical information for the GSE78220 cohort were obtained from the Gene Expression Omnibus database (https://www.ncbi.nlm.nih.gov/geo/),[30] and gene expression data were transformed using log2(x+1).

Drug sensitivity analysis

Normalized gene expression data of 809 tumor cell lines and response data for each cell line to 198 compounds were downloaded from the Genomics of Drug Sensitivity in Cancer database,[82] and the drug response data were converted to IC_{50} values. Spearman's correlations between cuproptosis activity and IC_{50} values for each drug were subsequently calculated, and only drugs with absolute values of correlation coefficients > 0.1 and $P < 0.05$ were considered to be associated with cuproptosis. The target data of the drugs were then matched with those of the screened drugs.

Declarations

Acknowledgements

This study was supported by Grants from the National Natural Science Foundation of China (No. 82172834) and the Natural Science Foundation of Changsha (kq2202375).

Author Contributions

C.W conceived the study, performed the literature search and bioinformatics analysis, and prepared the figures and manuscript; J.T, C.Q, Y.L and Y.P helped with data collection, analysis, and interpretation. X.W and W.L analyzed data and revised the manuscript; Q.L helped conceive this research and revise the manuscript. All authors read and approved the final manuscript.

Conflict of Interest

The authors declared no potential conflicts of interest.

References

1. Maung, M. T. et al. The molecular and cellular basis of copper dysregulation and its relationship with human pathologies. FASEB J. 35, e21810 (2021).
2. Dolmella, A. & Bandoli, G. The biological chemistry of the elements. The inorganic chemistry of life. Inorganica Chimica Acta 211, (1993).
3. Festa, R. A. & Thiele, D. J. Copper: An essential metal in biology. Curr. Biol. 21, (2011).
4. Linder, M. C. & Hazegh-Azam, M. Copper biochemistry and molecular biology. Am. J. Clin. Nutr. 63, 694–701 (1996).
5. Shiva, S. et al. Ceruloplasmin is a NO oxidase and nitrite synthase that determines endocrine NO homeostasis. Nat. Chem. Biol. 2, 486–493 (2006).
6. Moriya, M. et al. Copper is taken up efficiently from albumin and α2- macroglobulin by cultured human cells by more than one mechanism. Am. J. Physiol. - Cell Physiol. 295, (2008).
7. Babak, M. V. & Ahn, D. Modulation of intracellular copper levels as the mechanism of action of anticancer copper complexes: Clinical relevance. Biomedicines 9, (2021).
8. Kim, B. E., Nevitt, T. & Thiele, D. J. Mechanisms for copper acquisition, distribution and regulation. Nat. Chem. Biol. 4, 176–185 (2008).
9. Ruiz, L. M., Libedinsky, A. & Elorza, A. A. Role of Copper on Mitochondrial Function and Metabolism. Front. Mol. Biosci. 8, (2021).
10. Rossi, L., Lombardo, M. F., Ciriolo, M. R. & Rotilio, G. Mitochondrial Dysfunction in Neurodegenerative Diseases Associated with Copper Imbalance. Neurochem. Res. 29, 493–504 (2004).
11. Lu, J. & Holmgren, A. New roles for copper metabolism in cell proliferation, signaling, and disease. J. Biol. Chem. 284, 717–721 (2009).
12. Feng, Y. et al. Serum copper and zinc levels in breast cancer: A meta-analysis. J. Trace Elem. Med. Biol. 62, (2020).
13. Zabłocka-Słowińska, K. et al. Serum and whole blood Zn, Cu and Mn profiles and their relation to redox status in lung cancer patients. J. Trace Elem. Med. Biol. 45, 78–84 (2018).
14. Ebara, M. et al. Relationship between copper, zinc and metallothionein in hepatocellular carcinoma and its surrounding liver parenchyma. J. Hepatol. 33, 415–422 (2000).
15. Rizvi, A., Farhan, M., Naseem, I. & Hadi, S. M. Calcitriol–copper interaction leads to non enzymatic, reactive oxygen species mediated DNA breakage and modulation of cellular redox scavengers in hepatocellular carcinoma. Apoptosis 21, 997–1007 (2016).
16. Lavilla, I., Costas, M., Miguel, P. S., Millos, J. & Bendicho, C. Elemental fingerprinting of tumorous and adjacent non-tumorous tissues from patients with colorectal cancer using ICP-MS, ICP-OES and chemometric analysis. BioMetals 22, 863–875 (2009).

17. Lelièvre, P., Sancey, L., Coll, J. L., Deniaud, A. & Busser, B. The multifaceted roles of copper in cancer: A trace metal element with dysregulated metabolism, but also a target or a bullet for therapy. Cancers (Basel). 12, 1–25 (2020).
18. Blockhuys, S., Malmberg, P. & Wittung-Stafshede, P. Copper distribution in breast cancer cells detected by time-of-flight secondary ion mass spectrometry with delayed extraction methodology. Biointerphases 13, 06E412 (2018).
19. Moriguchi, M. et al. The copper chelator trientine has an antiangiogenic effect against hepatocellular carcinoma, possibly through inhibition of interleukin-8 production. Int. J. Cancer 102, 445–452 (2002).
20. Brady, D. C., Crowe, M. S., Greenberg, D. N. & Counter, C. M. Copper chelation inhibits BRAFV600E-driven melanomagenesis and counters resistance to BRAFV600E and MEK1/2 inhibitors. Cancer Res. 77, 6240–6252 (2017).
21. Tardito, S. et al. Copper binding agents acting as copper ionophores lead to caspase inhibition and paraptotic cell death in human cancer cells. J. Am. Chem. Soc. 133, 6235–6242 (2011).
22. Allensworth, J. L. et al. Disulfiram (DSF) acts as a copper ionophore to induce copper-dependent oxidative stress and mediate anti-tumor efficacy in inflammatory breast cancer. Mol. Oncol. 9, 1155–1168 (2015).
23. Jiao, Y., Hannafon, B. N., Zhang, R. R., Fung, K. M. & Ding, W. Q. Docosahexaenoic acid and disulfiram act in concert to kill cancer cells: A mutual enhancement of their anticancer actions. Oncotarget 8, 17908–17920 (2017).
24. Nuran Ercal, B. S. P., Hande Gurer-Orhan, B. S. P. & Nukhet Aykin-Burns, B. S. P. Toxic Metals and Oxidative Stress Part I: Mechanisms Involved in Me-tal induced Oxidative Damage. Curr. Top. Med. Chem. 1, 529–539 (2005).
25. Burton, G. J. & Jauniaux, E. Oxidative stress. Best Pract. Res. Clin. Obstet. Gynaecol. 25, 287–299 (2011).
26. Tsvetkov, P. et al. Copper induces cell death by targeting lipoylated TCA cycle proteins. Science (80-.). 375, 1254–1261 (2022).
27. Tang, D., Chen, X. & Kroemer, G. Cuproptosis: a copper-triggered modality of mitochondrial cell death. Cell Res. 32, 417–418 (2022).
28. Beroukhim, R. et al. The landscape of somatic copy-number alteration across human cancers. Nature 463, 899–905 (2010).
29. Hänzelmann, S., Castelo, R. & Guinney, J. GSVA: Gene set variation analysis for microarray and RNA-Seq data. BMC Bioinformatics 14, (2013).
30. Hugo, W. et al. Genomic and Transcriptomic Features of Response to Anti-PD-1 Therapy in Metastatic Melanoma. Cell 165, 35–44 (2016).
31. Bailey, P. et al. Genomic analyses identify molecular subtypes of pancreatic cancer. Nature 531, 47–52 (2016).

32. Saghafinia, S., Mina, M., Riggi, N., Hanahan, D. & Ciriello, G. Pan-Cancer Landscape of Aberrant DNA Methylation across Human Tumors. Cell Rep. 25, 1066–1080.e8 (2018).
33. Lee, D. D., Komosa, M., Nunes, N. M. & Tabori, U. DNA methylation of the TERT promoter and its impact on human cancer. Curr. Opin. Genet. Dev. 60, 17–24 (2020).
34. Bartel, D. P. MicroRNAs: Target Recognition and Regulatory Functions. Cell 136, 215–233 (2009).
35. Wu, C. et al. LINC00470 promotes tumour proliferation and invasion, and attenuates chemosensitivity through the LINC00470/miR-134/Myc/ABCC1 axis in glioma. J. Cell. Mol. Med. 24, 12094–12106 (2020).
36. Yao, R. W., Wang, Y. & Chen, L. L. Cellular functions of long noncoding RNAs. Nat. Cell Biol. 21, 542–551 (2019).
37. Chiu, H. S. et al. Pan-Cancer Analysis of lncRNA Regulation Supports Their Targeting of Cancer Genes in Each Tumor Context. Cell Rep. 23, 297–312.e12 (2018).
38. Bushweller, J. H. Targeting transcription factors in cancer — from undruggable to reality. Nat. Rev. Cancer 19, 611–624 (2019).
39. Liberzon, A. et al. The Molecular Signatures Database Hallmark Gene Set Collection. Cell Syst. 1, 417–425 (2015).
40. Thorsson, V. et al. The Immune Landscape of Cancer. Immunity 48, 812–830.e14 (2018).
41. Zeng, D. et al. Tumor microenvironment characterization in gastric cancer identifies prognostic and immunotherapeutically relevant gene signatures. Cancer Immunol. Res. 7, 737–750 (2019).
42. Pardoll, D. M. The blockade of immune checkpoints in cancer immunotherapy. Nat. Rev. Cancer 12, 252–264 (2012).
43. Ribas, A. & Wolchok, J. D. Cancer immunotherapy using checkpoint blockade. Science (80-.). 359, 1350–1355 (2018).
44. Mariathasan, S. et al. TGFβ attenuates tumour response to PD-L1 blockade by contributing to exclusion of T cells. Nature 554, 544–548 (2018).
45. Bandmann, O., Weiss, K. H. & Kaler, S. G. Wilson's disease and other neurological copper disorders. Lancet Neurol. 14, 103–113 (2015).
46. Gaggelli, E., Kozlowski, H., Valensin, D. & Valensin, G. Copper homeostasis and neurodegenerative disorders (Alzheimer's, prion, and Parkinson's diseases and amyotrophic lateral sclerosis). Chem. Rev. 106, 1995–2044 (2006).
47. Ge, E. J. et al. Connecting copper and cancer: from transition metal signalling to metalloplasia. Nat. Rev. Cancer 22, 102–113 (2022).
48. O'Day, S. J. et al. Final results of phase III SYMMETRY study: Randomized, double-blind trial of elesclomol plus paclitaxel versus paclitaxel alone as treatment for chemotherapy-naive patients with advanced melanoma. J. Clin. Oncol. 31, 1211–1218 (2013).
49. O'Day, S. et al. Phase II, randomized, controlled, double-blinded trial of weekly elesclomol plus paclitaxel versus paclitaxel alone for stage IV metastatic melanoma. J. Clin. Oncol. 27, 5452–5458

(2009).
50. Cen, D., Brayton, D., Shahandeh, B., Meyskens, F. L. & Farmer, P. J. Disulfiram facilitates intracellular Cu uptake and induces apoptosis in human melanoma cells. J. Med. Chem. 47, 6914–6920 (2004).
51. Schreiber, M., Muller, W. J., Singh, G. & Graham, F. L. Comparison of the effectiveness of adenovirus vectors expressing cyclin kinase inhibitors p16(INK4A), p18(INK4C), p19(INK4D), p21(WAF1/CIP1) and p27(KIP1) in inducing cell cycle arrest, apoptosis and inhibition of tumorigenicity. Oncogene 18, 1663–1676 (1999).
52. Herbig, U., Jobling, W. A., Chen, B. P. C., Chen, D. J. & Sedivy, J. M. Telomere shortening triggers senescence of human cells through a pathway involving ATM, p53, and p21CIP1, but not p16INK4a. Mol. Cell 14, 501–513 (2004).
53. Heidenreich, A., Gaddipati, J. P., Moul, J. W. & Srivastava, S. Molecular analysis of P16(Ink4)/CDKN2 and P15(Ink4B)/MTS2 genes in primary human testicular germ cell tumors. J. Urol. 159, 1725–1730 (1998).
54. Nobori, T. et al. Deletions of the cyclin-dependent kinase-4 inhibitor gene in multiple human cancers. Nature 368, 753–756 (1994).
55. Rocco, J. W. & Sidransky, D. p16(MTS-1/CDKN2/INK4a) in cancer progression. Exp. Cell Res. 264, 42–55 (2001).
56. Luo, J. P., Wang, J. & Huang, J. H. CDKN2A is a prognostic biomarker and correlated with immune infiltrates in hepatocellular carcinoma. Biosci. Rep. 41, (2021).
57. Kang, N. et al. Identification and validation of EMT-immune-related prognostic biomarkers CDKN2A, CMTM8 and ILK in colon cancer. BMC Gastroenterol. 22, 190 (2022).
58. Shi, W.-K., Li, Y.-H., Bai, X.-S. & Lin, G.-L. The Cell Cycle-Associated Protein CDKN2A May Promotes Colorectal Cancer Cell Metastasis by Inducing Epithelial-Mesenchymal Transition. Front. Oncol. 12, (2022).
59. Worst, T. S. et al. CDKN2A as transcriptomic marker for muscle-invasive bladder cancer risk stratification and therapy decision-making. Sci. Rep. 8, (2018).
60. Zhang, Z. et al. FDX1 can Impact the Prognosis and Mediate the Metabolism of Lung Adenocarcinoma. Front. Pharmacol. 12, 749134 (2021).
61. Gabriely, G. et al. Human glioma growth is controlled by microRNA-10b. Cancer Res. 71, 3563–3572 (2011).
62. Yan, L., Liu, Z., Yin, H., Guo, Z. & Luo, Q. Silencing of MEG3 inhibited ox-LDL-induced inflammation and apoptosis in macrophages via modulation of the MEG3/miR-204/CDKN2A regulatory axis. Cell Biol. Int. 43, 409–420 (2019).
63. Paraskevopoulou, M. D. & Hatzigeorgiou, A. G. Analyzing MiRNA–LncRNA interactions. Methods Mol. Biol. 1402, 271–286 (2016).
64. Zhang, H. et al. Transcription factor NFIC functions as a tumor suppressor in lung squamous cell carcinoma progression by modulating lncRNA CASC2. Cell Cycle 21, 63–73 (2022).

65. Lv, S., Liu, L., Yang, B. & Zhao, X. Association of miR-9-5p and NFIC in the progression of gastric cancer. Hum. Exp. Toxicol. 41, 096032712210846 (2022).
66. Chen, F. et al. MCPIP1-mediated NFIC alternative splicing inhibits proliferation of triple-negative breast cancer via cyclin D1-Rb-E2F1 axis. Cell Death Dis. 12, (2021).
67. Liang, X., Gao, J., Wang, Q., Hou, S. & Wu, C. ECRG4 Represses Cell Proliferation and Invasiveness via NFIC/OGN/NF-κB Signaling Pathway in Bladder Cancer. Front. Genet. 11, (2020).
68. Wang, H., Shi, X. & Wu, S. miR-550a-3/NFIC plays a driving role in esophageal squamous cell cancer cells proliferation and metastasis partly through EMT process. Mol. Cell. Biochem. 472, 115–123 (2020).
69. Xu, G. et al. LBX2-AS1 up-regulated by NFIC boosts cell proliferation, migration and invasion in gastric cancer through targeting miR-491-5p/ZNF703. Cancer Cell Int. 20, (2020).
70. Zhang, H. et al. Disulfiram treatment facilitates phosphoinositide 3-kinase inhibition in human breast cancer cells in vitro and in vivo. Cancer Res. 70, 3996–4004 (2010).
71. Martinez-Outschoorn, U. E., Peiris-Pagés, M., Pestell, R. G., Sotgia, F. & Lisanti, M. P. Cancer metabolism: A therapeutic perspective. Nat. Rev. Clin. Oncol. 14, 11–31 (2017).
72. Carracedo, A., Cantley, L. C. & Pandolfi, P. P. Cancer metabolism: Fatty acid oxidation in the limelight. Nat. Rev. Cancer 13, 227–232 (2013).
73. Leone, R. D. & Powell, J. D. Metabolism of immune cells in cancer. Nat. Rev. Cancer 20, 516–531 (2020).
74. Rooney, M. S., Shukla, S. A., Wu, C. J., Getz, G. & Hacohen, N. Molecular and genetic properties of tumors associated with local immune cytolytic activity. Cell 160, 48–61 (2015).
75. Fridman, W. H., Zitvogel, L., Sautès-Fridman, C. & Kroemer, G. The immune contexture in cancer prognosis and treatment. Nat. Rev. Clin. Oncol. 14, 717–734 (2017).
76. Li, B., Cui, Y., Nambiar, D. K., Sunwoo, J. B. & Li, R. The immune subtypes and landscape of squamous cell carcinoma. Clin. Cancer Res. 25, 3528–3537 (2019).
77. Xiao, Q. et al. Genetic and epigenetic biomarkers of immune checkpoint blockade response. J. Clin. Med. 9, 286 (2020).
78. Wilkerson, M. D. & Hayes, D. N. ConsensusClusterPlus: a class discovery tool with confidence assessments and item tracking. Bioinformatics 26, 1572–1573 (2010).
79. Ye, Y. et al. Characterization of hypoxia-associated molecular features to aid hypoxia-targeted therapy. Nat. Metab. 1, 431–444 (2019).
80. Knijnenburg, T. A. et al. Genomic and Molecular Landscape of DNA Damage Repair Deficiency across The Cancer Genome Atlas. Cell Rep. 23, 239–254.e6 (2018).
81. Yoshihara, K. et al. Inferring tumour purity and stromal and immune cell admixture from expression data. Nat. Commun. 4, (2013).
82. Yang, W. et al. Genomics of Drug Sensitivity in Cancer (GDSC): A resource for therapeutic biomarker discovery in cancer cells. Nucleic Acids Res. 41, (2013).

Figures

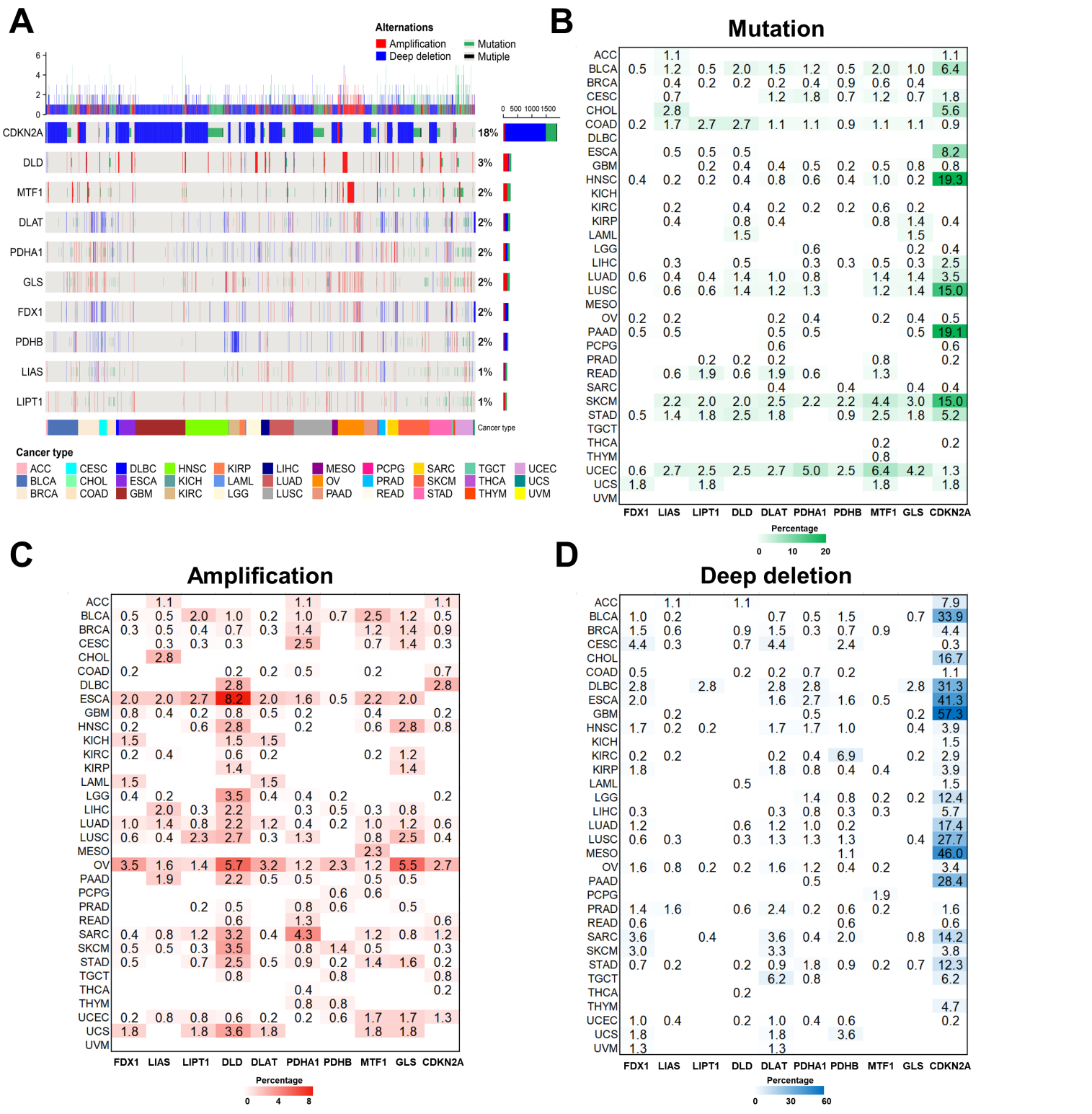

Figure 1

The somatic alterations of cuproptosis regulators in cancer. A Landscape of somatic alterations (SNV and SCNA) of cuproptosis regulators in cancer. Each row represents a gene, and each column represents a patient. The frequency of alterations of 10 cuproptosis regulators are presented. Only patients with

somatic alterations in the cuproptosis regulators are shown. Alteration rates per gene are displayed in the right labels. **B-D** Distribution of mutation (**B**), amplification (**C**) and deep deletion (**D**) frequencies over cancer types. The numbers in the graph represent the specific frequency values. The intensity of color is proportional to the frequency.

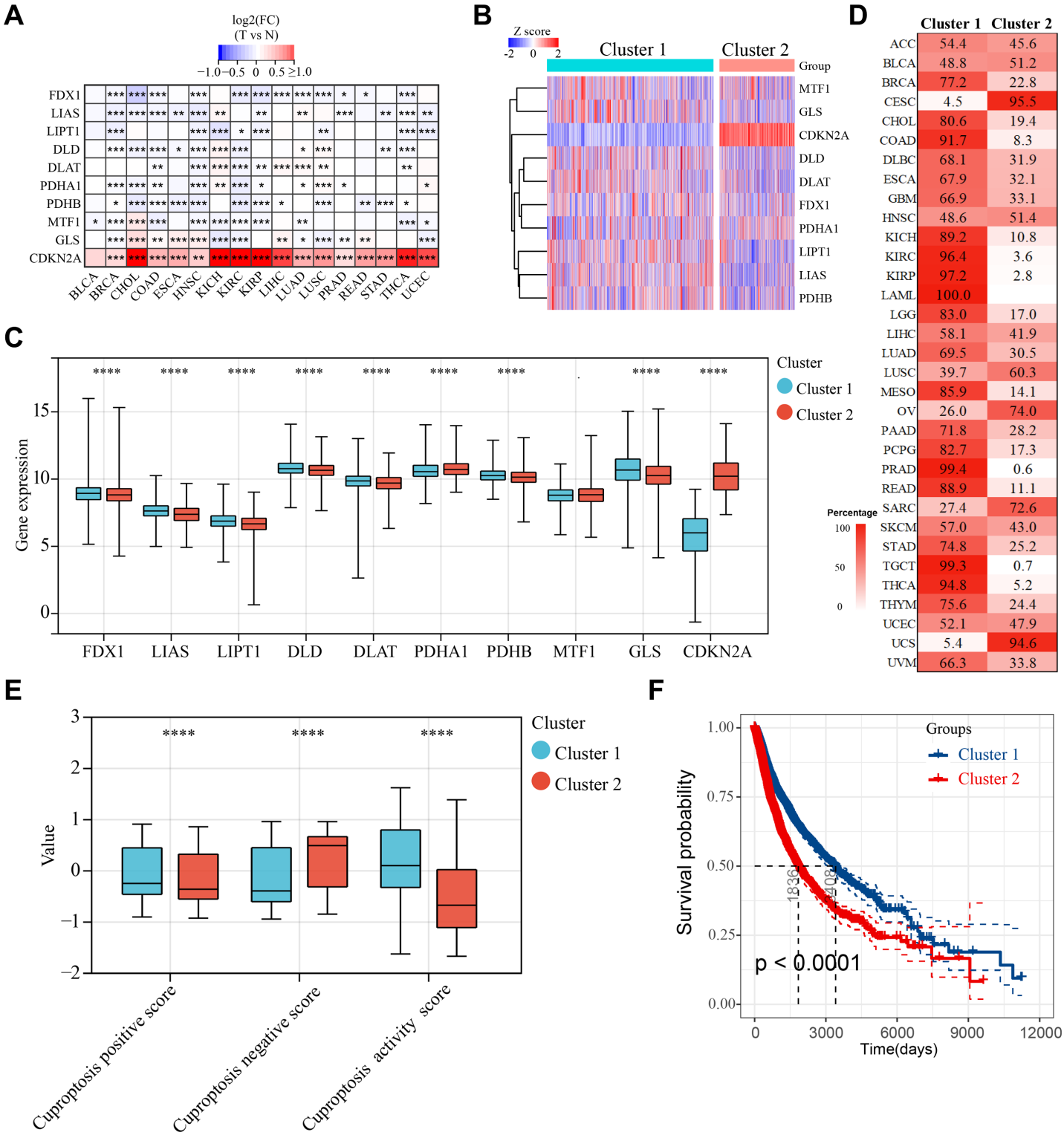

Figure 2

Gene expression patterns of cuproptosis regulators. A The mRNA differences between tumor samples and adjacent normal samples. Red indicates high expression in tumor, and blue indicates low expression. * $P < 0.05$, ** $P < 0.01$, *** $P < 0.001$. **B** Unsupervised consensus clustering of cuproptosis regulators expression revealed two distinct clusters. Each row represents a cuproptosis regulator, and each column is a patient. Red indicates high expression, and blue indicates low expression. The expression data were normalized by z-score. **C** Boxplots showing the differences of 10 cuproptosis regulators in the two clusters. The differences were tested by Student's t test. **** $P < 0.0001$. **D** Sample distribution in the two clusters. Each row represents a cancer type, and each column represents a cluster. The number and the red intensity in each box show the percentage of samples classified in the corresponding cluster. **E** Boxplots showing the differences of cuproptosis positive score, cuproptosis negative score and cuproptosis activity score in the two clusters. The differences were tested by Student's t test. **** $P < 0.0001$. **F** The Kaplan–Meier curve showing the difference in OS between Cluster 1 and Cluster 2. Cluster 1 is indicated in blue line and Cluster 2 in red.

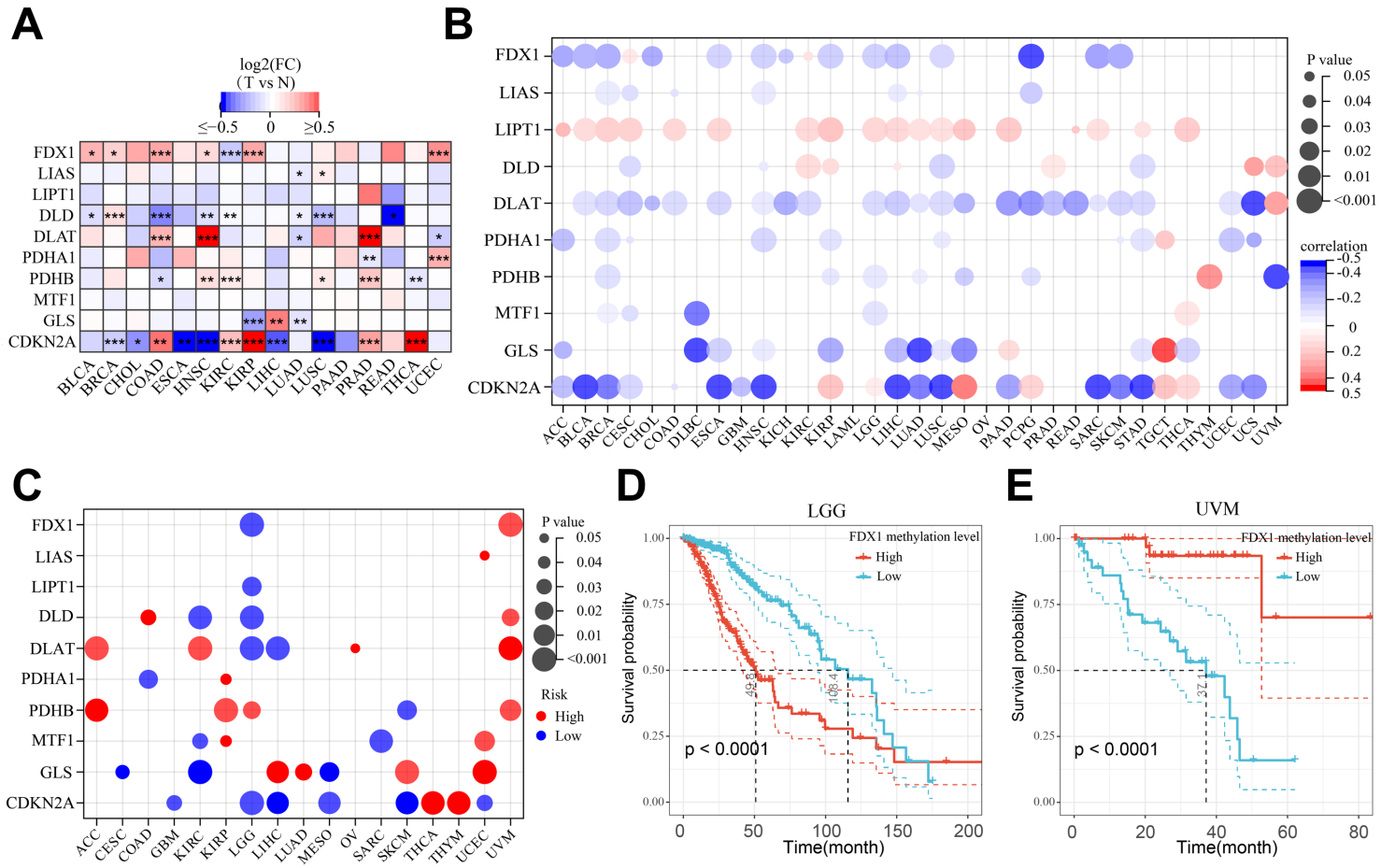

Figure 3

Methylation of cuproptosis regulators. A The methylation differences between tumor samples and adjacent normal samples. Red indicates increased methylation in tumor, and blue indicates decreased methylation. * $P < 0.05$, ** $P < 0.01$, *** $P < 0.001$. **B** Correlation between methylation and mRNA gene expression. Blue points represent a negative correlation and red points represent a positive correlation,

where the darker of color, the higher the correlation. **C** Relationship between cuproptosis regulators methylation and survival in cancer. Red dots indicate that hypermethylation is associated with worse survival and blue dots indicate that hypermethylation is associated with better survival. The size of the point represents the statistical significance, where the larger the dot size, the higher the statistical significance. Only tumor types with significance are shown. **D,E** Kaplan–Meier curves showing the difference in OS between FDX1 hypermethylation group and FDX1 hypomethylation group in LGG (**D**) and UVM (**E**). Hypermethylation group is indicated in red line and hypomethylation group in blue.

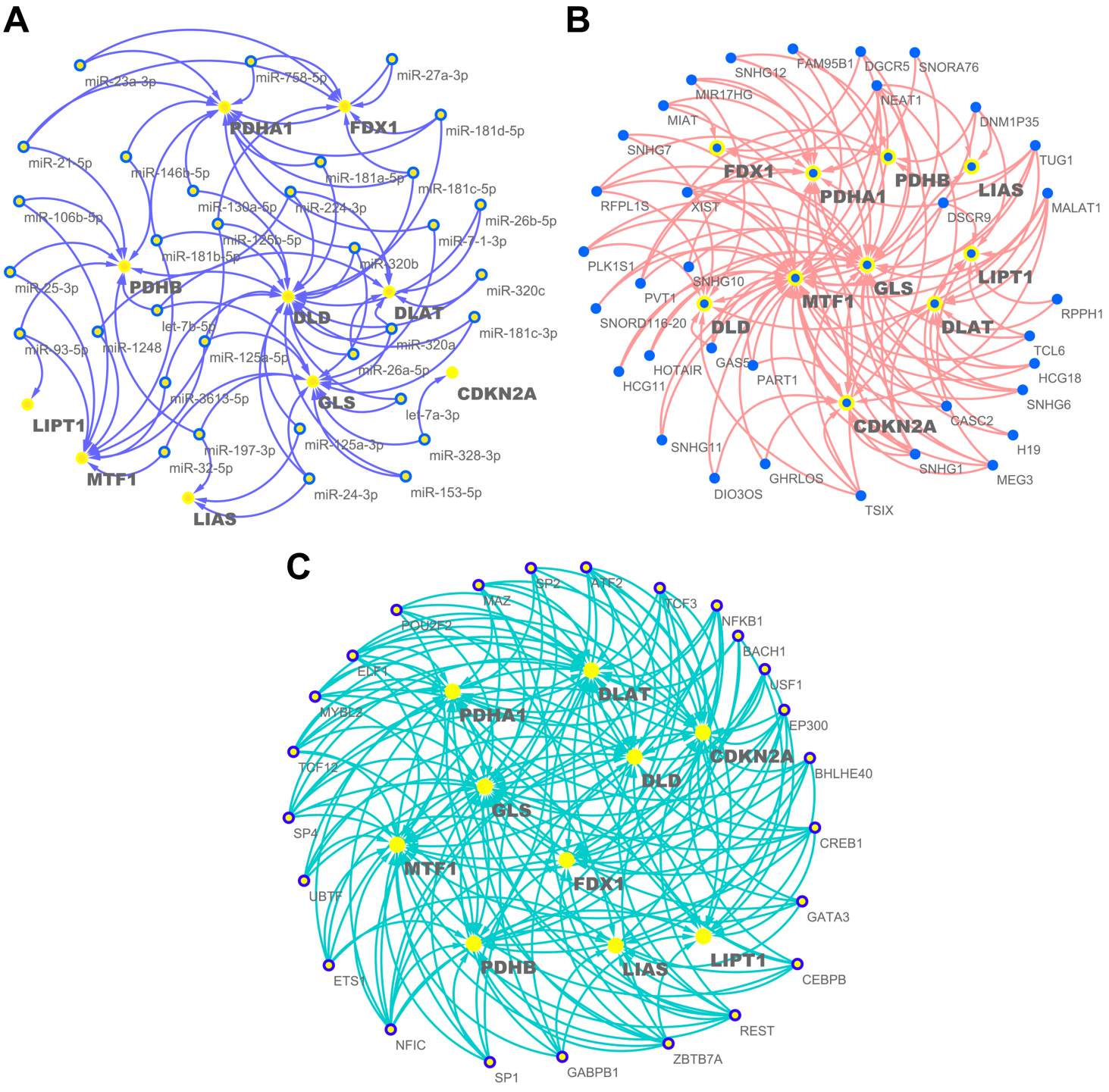

Figure 4

miRNA, lncRNA and TF regulatory networks. A The miRNA–mRNA regulatory network showing miRNAs target at least two cuproptosis regulators. **B** The lncRNA–mRNA regulatory network showing lncRNAs target at least two cuproptosis regulators. **C** The TF–mRNA regulatory network showing TFs target at least five cuproptosis regulators.

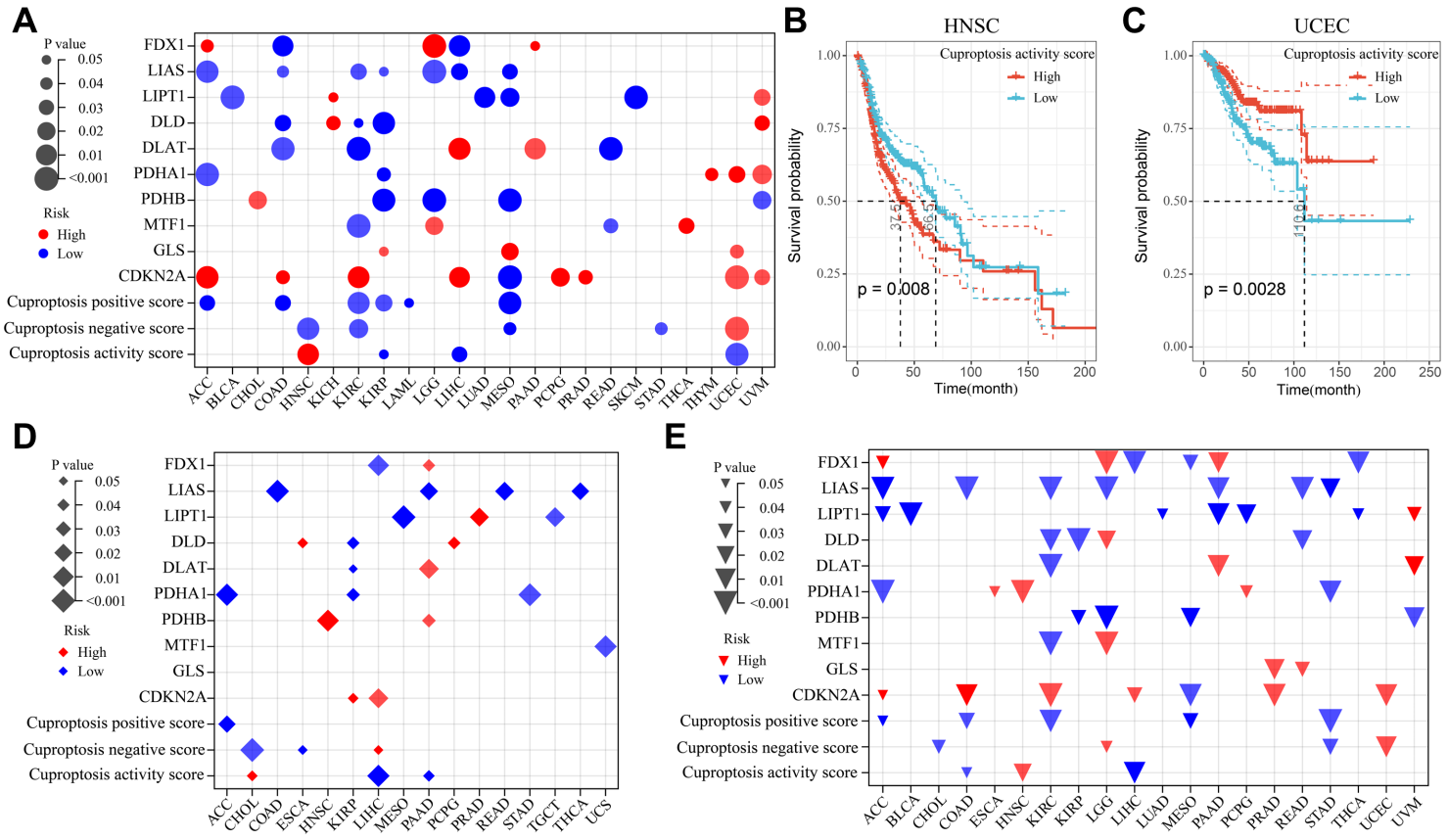

Figure 5

Prognostic value of cuproptosis. A,D,E OS (**A**), DFI (**D**) and PFI (**E**) analyses of cuproptosis regulators and cuproptosis scores. The dot size represents the significance of the effects of cuproptosis regulators or scores on survival in each cancer type, the p-value was obtained from a log-rank test. Only tumor types with significance are shown. Red dots indicate that the high gene expression or high score is associated with worse survival and blue dots indicate that the high gene expression or high score is associated with better survival. B,C Kaplan–Meier curves showing the difference in OS between high cuproptosis activity score group and low cuproptosis activity score group in HNSC (**B**) and UCEC (**C**). High cuproptosis activity score group is indicated in red line and low cuproptosis activity score group in blue.

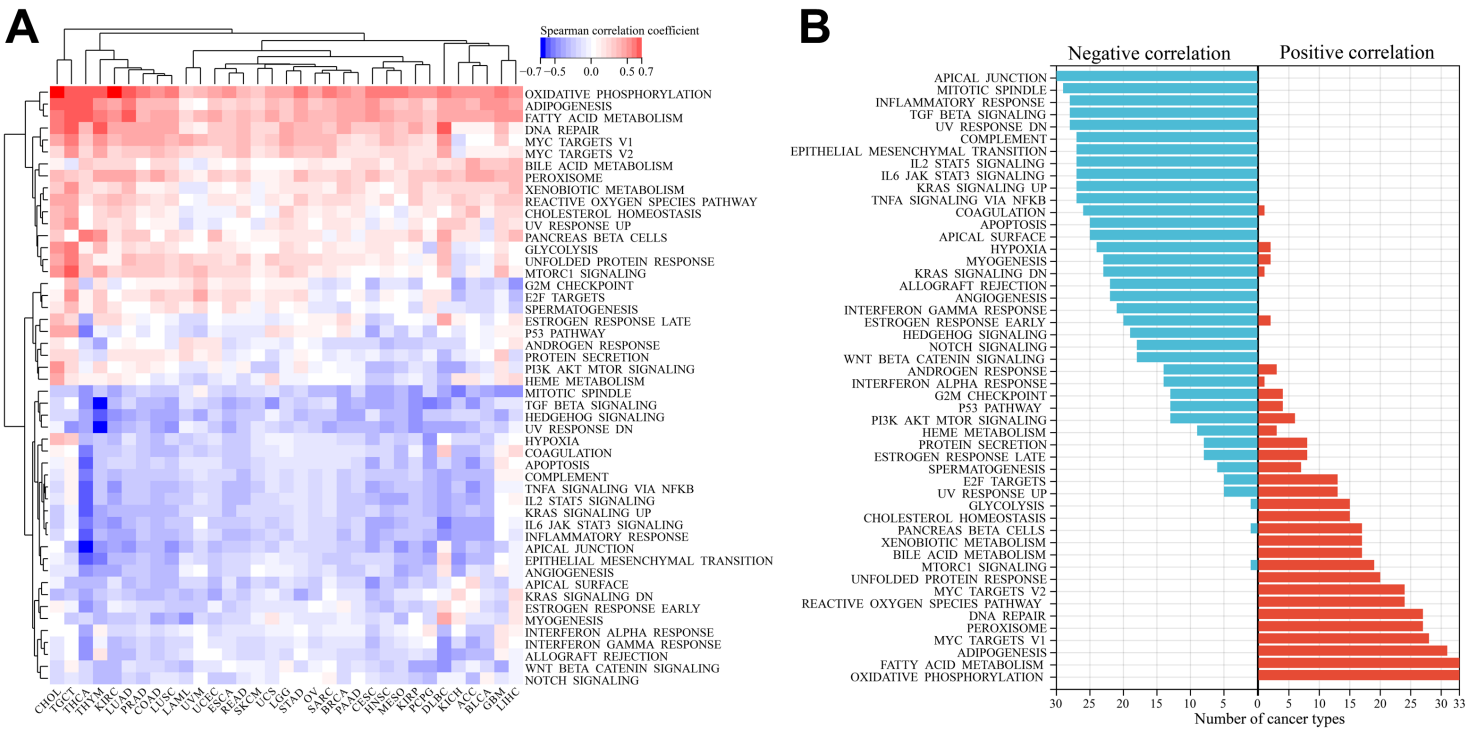

Figure 6

Cuproptosis correlated hallmark pathways in cancer. A The heatmap showing the correlation between cuproptosis activity and hallmark pathway activity in each cancer type. Each column is a cancer type, and each row is a hallmark set. Red represents positive correlation, blue represents negative correlation. Unsupervised clustering used Euclidean distance metric with complete linkage. **B** Bar plots showing number of cancer types having negative (blue) and positive (red) correlations between cuproptosis activity and hallmark pathways.

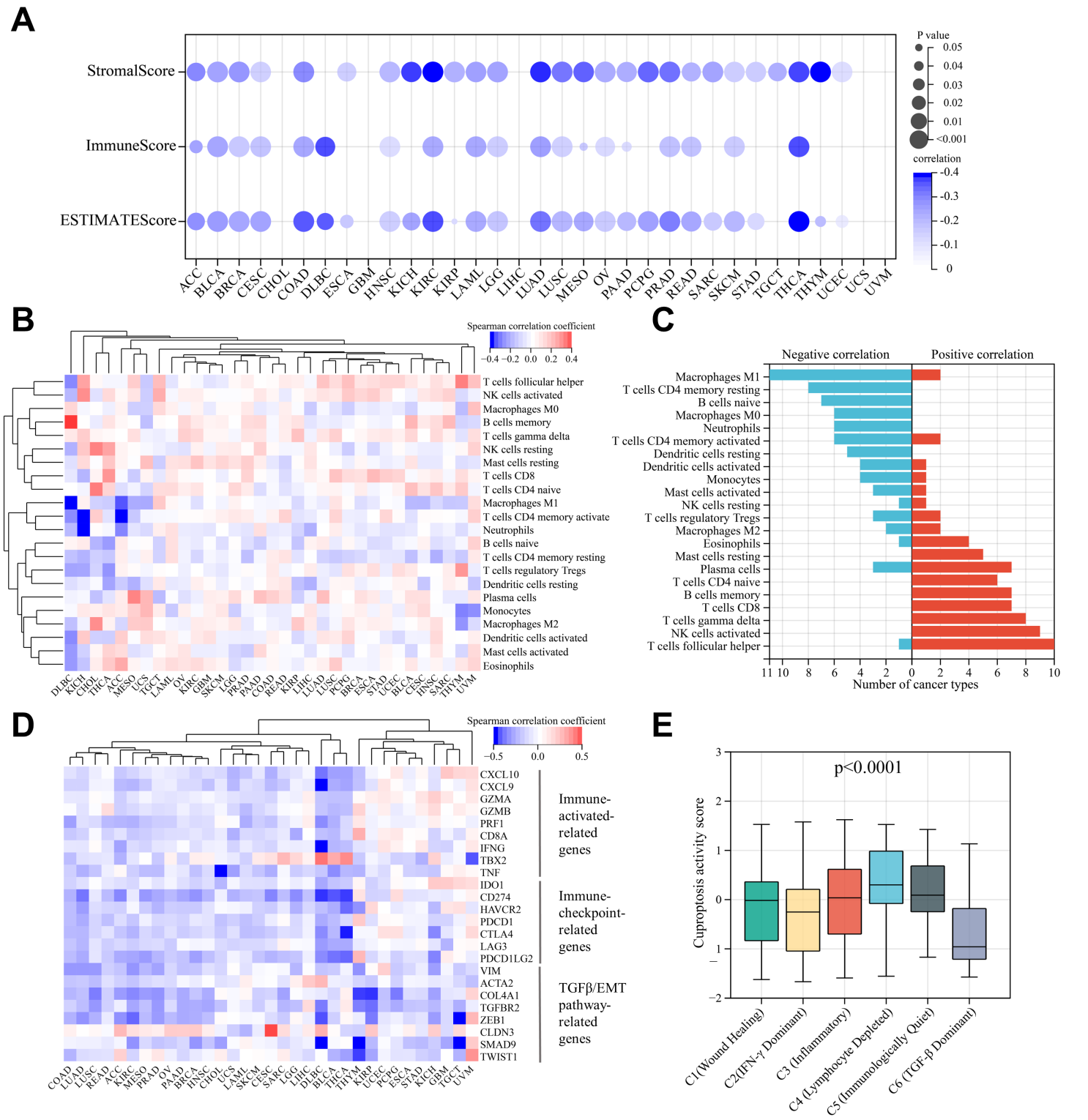

Figure 7

Cuproptosis correlates with tumor immune characteristics. A Correlation between cuproptosis activity and ImmuneScore, StromalScore and ESTIMATEScore. Blue points represent a negative correlation, where the darker of color, the higher the correlation. **B** The heatmap showing the correlation between cuproptosis activity and the abundance of 22 immune cells in each cancer type. Each column is a cancer type, and each row is an immune cell. Red represents positive correlation, blue represents negative correlation.

Unsupervised clustering used Euclidean distance metric with complete linkage. **C** Bar plots showing number of cancer types having negative (blue) and positive (red) correlations between cuproptosis activity and 22 immune cells. **D** The heatmap showing the correlation between cuproptosis activity and immunomodulator expression in each cancer type. Each column is a cancer type, and each row is an immunomodulator. Red represents positive correlation, blue represents negative correlation. Unsupervised clustering used Euclidean distance metric with complete linkage. **E** Boxplots represent the differences in cuproptosis activity between immune subtypes (C1-C6). The Student's t test was used for the comparison between two immune subtypes. All comparison *P*<0.0001.

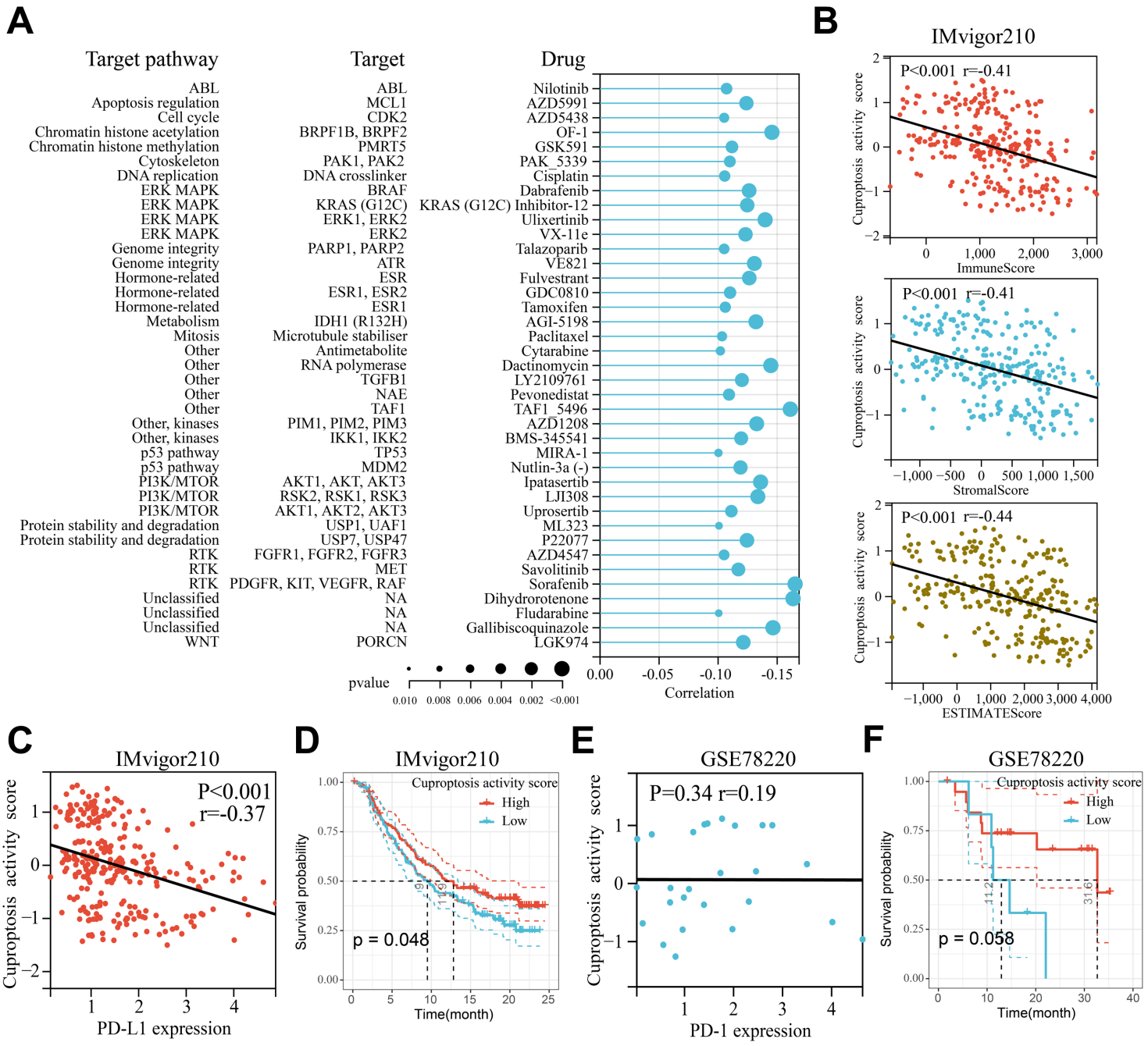

Figure 8

The relationship between cuproptosis activity and drug sensitivity and immunotherapy outcome. A The correlation between cuproptosis activity and drug sensitivity (IC50 value). Each row represents a drug and drug targets. The length of the line represents the correlation coefficient. The blue represents a negative correlation, that is, high cuproptosis activity correlates with higher drug sensitivity. The size of the point represents the statistical significance, where the larger the dot size, the higher the statistical significance. **B** Correlation of cuproptosis activity with ImmuneScore, StromalScore and ESTIMATEScore in the IMvigor210 cohort. **C** Correlation of cuproptosis activity with PD-L1 expression in the IMvigor210 cohort. **D** Kaplan-Meier curve depict the OS difference between high and low cuproptosis activity groups after anti-PD-L1 immunotherapy in the IMvigor210 cohort. **E** Correlation of cuproptosis activity with PD-1 expression in the GSE78220 cohort. **F** Kaplan-Meier curve depict the OS difference between high and low cuproptosis activity groups after anti-PD-1 immunotherapy in the GSE78220 cohort. Statistical significance was assessed by a log-rank test.

Supplementary Files

This is a list of supplementary files associated with this preprint. Click to download.

- FigureS1.tif
- FigureS2.tif
- FigureS3.tif
- FigureS4.tif
- FigureS5.tif
- FigureS6.tif
- TableS1.xlsx
- TableS2.xlsx
- TableS3.xlsx
- TableS4.xlsx
- TableS5.xlsx
- TableS6.xlsx
- TableS7.xlsx
- TableS8.xlsx
- TableS9.xlsx